JETIR.ORG ISSN: 2349-5162 | ESTD Year : 2014 | Monthly Issue
JOURNAL OF EMERGING TECHNOLOGIES AND INNOVATIVE RESEARCH (JETIR)
An International Scholarly Open Access, Peer-reviewed, Refereed Journal

Modeling Fracture Behavior in Fiber-Reinforced Polymer Composites at Multiple Scales

[1]A. Behera, [1]Tanisha Ipsita Hota, [1] Asish kumar sahoo, [1]P. Das, [1]G. Barik
[1]Asst. Professor, Department of Mechanical Engineering, GITAM, Bhubaneswar

Abstract:

Fiber-reinforced polymer matrix composites (FRPMCs) often undergo intra-laminar fiber-matrix fracture, commonly known as splitting, under tensile loading. Numerical modeling faces challenges in predicting this failure mode and its effect on a macroscopically homogenized model. We propose an effective two-scale modeling approach that integrates the micromechanics 2-concentric cylinder (2CYL) analytical technique to capture pre-peak nonlinearity and the 3D orthotropic smeared crack approach (SCA) to simulate post-peak softening behavior. By using typical 3D finite elements, we represent a homogenized ply that explicitly considers matrix fracture concerning the ply angle orientation. We demonstrate the method's capability by predicting grip-to-grip longitudinal splitting in a 00 ply, mixed-mode matrix cracking in a 450 ply, transverse matrix cracking in a 900 ply, and the failure of the laminate comprising these plies. Our results indicate that our proposed approach closely aligns with experimental findings.

Introduction

Numerous researchers have conducted experiments and observed the phenomenon of intralaminar fiber-matrix splitting failure [6–9]. In laminated composites, this failure mechanism is significant, and using a validated computational tool is essential when designing with FRPMCs. Despite significant efforts towards modeling progressive failure, replicating the vast number of matrix fractures observed in studies [10–15] remains challenging. Each ply consists of numerous fibers encased in a matrix material and arranged in various configurations. Under local stress conditions, the matrix within the ply and between the fibers develops micro-fractures; however, these cracks do not propagate rapidly due to the fibers preventing their growth. These matrix micro-cracks contribute to the pre-peak nonlinear behavior of the lamina. Over time, they may evolve into a single macro-crack, leading to the failure of an individual ply.

When studying larger structures, modeling individual fibers computationally is costly. However, it's feasible to model fibers and matrix individually at a microscopic representative volume element (RVE) level [16–22]. Additionally, numerical simulations can be conducted to capture this failure behavior. Nevertheless, as demonstrated in this article, a two-scale model of a homogenized lamina is capable of accurately representing the fiber-matrix failure mode. Furthermore, when this foundational modeling approach for a lamina is utilized in a three-dimensional model of a laminate, it is also observed to accurately predict laminate failure. As a result, the modeling approach that is presented here can be utilized for predictive modeling. The author who corresponds. electronic mail address: awaas@umich.edu (A.M. Waas), which will result in a considerable decrease in the number of tests that are required, which will in turn lead to a significant cost savings.

Fiber-reinforced polymers are becoming more essential materials for structural applications across a wide range of industries. In the field of civil engineering, for instance, there are a number of noteworthy uses of unidirectional (UD) carbon fiber reinforced polymers (CFRP) [1,2,3,4]. There are a number of mathematical regimes that have been developed in order to estimate the strength of these materials [9]. These regimes include analytical [5,6], semi- analytical [7], and numerical models [8]. As a result of the fact that homogenized macroscale models [10] are unable to accurately reflect the failure processes of a composite material, micromechanical models have been created as an alternative [11]. Phenomenological models, such as shear lag

and fiber bundle models [12], and numerical models that make use of the finite element method (FEM) [9] are two categories that may be taken into consideration when discussing micromechanical models. Although both kinds of micromechanical models take into consideration the interactions between fiber and matrix, only numerical models have the capacity to completely represent the complex nature of damage progression in composites [13]. This is because numerical methods describe the interactions between the matrix and the fiber. They are able to provide a realistic description of the process by which failure develops, as well as the manner in which flaws that are relatively minor in comparison to the microstructural characteristics influence the performance of a composite. When it comes to creating laminates, numerical micromodels may also be used to address ply properties without the need for experimental investigations. A number of analytical models have been devised for the purpose of solving the homogenized properties based on the characteristics of the component entities [14]. On the other hand, the analytical models may not always operate in a reliable manner, particularly in situations when the fiber volume percentages are more than 0.6 [15]. The analytical answers, on the other hand, are quite easy to implement. For the purpose of computing mechanical finite element models, these homogenized macroscopic material characteristics are required as an input. Micromechanical modeling is important not only during the manufacture of a component but also throughout its service life. It is possible that it might give a way to mimic the reaction of a structure as a consequence of various sizes and kinds of damage that occur during service, and as a result, it could be incorporated into relevant condition monitoring systems. In addition to this, it enables continuous review and offers improved information on the measures that must be taken in the event that damage is discovered and defined via the use of non-destructive evaluation [16]. To put it another way, it improves the capability of determining the residual strength and determining whether or not a component may continue to be used in service. However, in order to provide findings that can be relied upon, micromechanical models need to have the appropriate input, which includes the characteristics of the fibers and matrix (also known as component qualities) as well as the microstructure.

Anisotropic composite materials pose several challenges, including obtaining component attributes and confirming homogenized products. However, for transversely isotropic materials like carbon fiber and unidirectional fiber-reinforced composites, only five material constants are independent of each other [17]. Determining the longitudinal Young's modulus of the fiber from instrumented tensile testing results is straightforward [18,19]. Additionally, the rule of mixing has been well-established for the axial characteristics of UD composites, facilitating the application of inverse micromechanics with confidence. Direct measurements of the transverse Young's modulus (E2f) have been conducted using nanoindentation [14], yielding values slightly higher than those obtained through various analytical inverse micromechanics solutions [20]. Carbon fiber's transverse Young's modulus has also been quantified using resonance frequencies [21].

However, obtaining the remaining three elastic constants of a single filament through experimental means is challenging. Many publications rely on inverse micromechanics and measurement of composite characteristics [22], while others reference difficult-to-access sources [25], or simply assume certain elastic qualities [22,23,24]. Some modeling works make straightforward assumptions about elastic properties.

The simulated microstructure should accurately describe parameters such as fiber volume percentage, packing, size, and shape to the greatest extent possible. Periodic square or hexagonal fiber packing, while idealized, is contrasted with random packing generators, which produce a more realistic distribution of fibers [26]. However, large fiber volume fractions pose a challenge for generators [27], and the difference between periodic and random packing affects transverse elastic constants [15]. Close proximity of fibers in strength models can lead to significant increases in stress concentration factors [26]. Nonetheless, the stress recovery distance is reduced as the matrix tends to be more rigid in the immediate area. Consequently, the type of packing does not significantly impact the uniaxial loading of UD CFRPs in the fiber direction [28]. However, debonding and matrix plasticity can alter findings [29], and off-axis loading requires random packing for accurate results [30The purpose of this study is to explain the process of developing a multiscale microstructure- based model and to validate that model via experimentation. At the end of the day, the purpose of this effort is to develop a macroscale strength model that takes into account microstructural faults without the requirement for experimental model update or calibration. The following is the outline of the contents of the paper: To begin, a description is given of the overall framework of the multiscale method as well as the prerequisites for a micromechanical model. The next step is to describe the numerical techniques that may be used to calculate the characteristics of composites by

making use of the information that was established in the previous stage. Lastly, the composite characteristics are used in order to acquire pertinent boundary conditions (BCs) for the purpose of loading the initial micromodel and modeling the impact that a defect has on the strength of the material. A comparison is made between the findings of the modeling and the measurements of a pultruded UD CFRP beam at each incremental stage.

1. Methods and Materials

A common multiscale method [31] is followed by the workflow, which is shown in Figure 1. In this technique, microscopic behavior is characterized by means of a representative volume element (RVE), and the first stage involves homogenization of the RVE in order to mimic the global reaction via simulation. By adjusting the size of the RVE until the homogenization of characteristics is achieved, a statistical volume element (SVE) is created. This allows for the evaluation of the statistical representation of the microstructure. Although not all of the individual input parameters are required fully known, the sensitivity of the homogenized qualities to changes in component properties, such as fiber and matrix properties, is analyzed with the purpose of determining the significance of each individual parameter. The purpose here is to avoid using experimental calibration [33] or inverse micromechanics, even if it is possible to measure homogenized qualities by experimentation [32]. This may be attributed to two different factors: To begin, every time an input parameter is altered, it is necessary to do experimental work, which may be both time-consuming and costly. Using inverse micromechanics or model calibration eliminates the need for experimental validation, which brings us to our second statement. A macroscopic model that takes into account the component geometry, boundary conditions, and load scenarios is the second phase in the process. This step involves inserting the homogenized characteristics into the model. By loading the component and comparing the observed strain values with the simulated strain, it is possible to provide experimental validation of the response of the macroscopic model. Identification of key locations within the structure is accomplished by the usage of the macroscopic model. In order to ensure that the displacements and boundary conditions for the RVE are applicable to the real application, the third stage in the workflow entails making use of the crucial locations for defining the RVE. Now, it is possible to analyze at microscale under stress conditions that are relevant to real-life applications the influence of known faults that were discovered using advanced non-destructive testing [16] or hypothetical defects. There is thus the possibility of calculating the simulated failure strength of a damaged component and comparing it to the failure loads that were acquired via experimentation. To get the best possible outcome, this procedure should enable the assessment of the residual strength of a damaged component based on the findings of an in-service inspection.

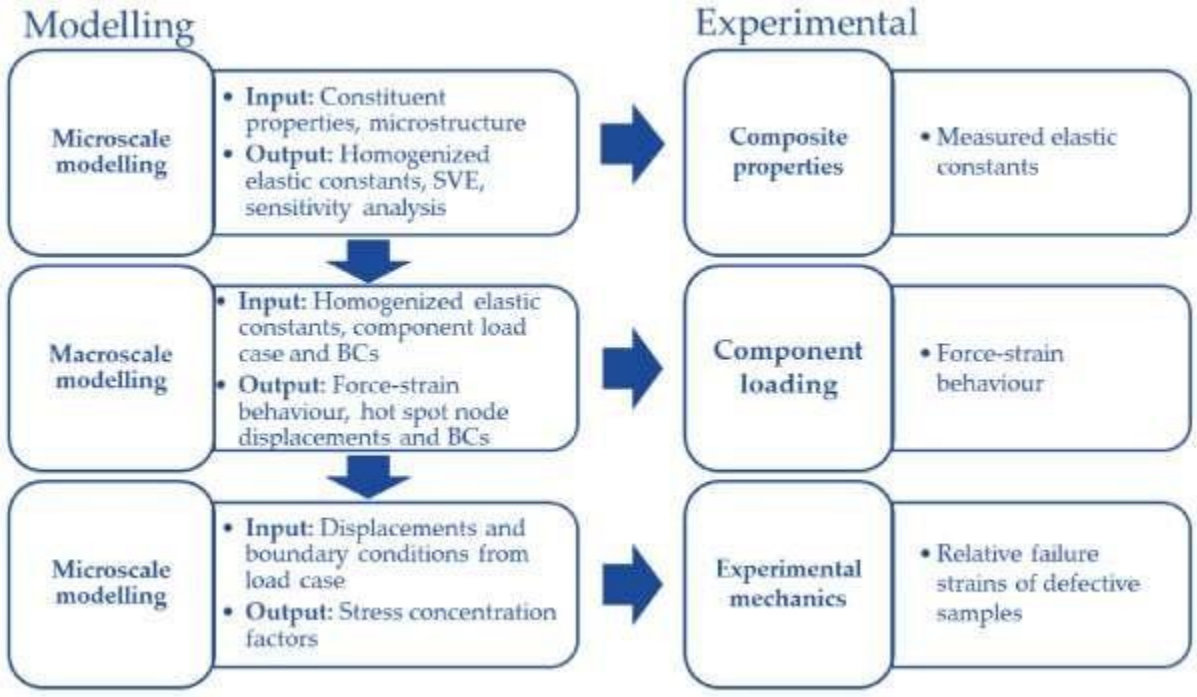

2. Proposed Mechanism

The three-point bending of a pultruded UD CFRP beam is the subject of the macroscopic model and case study research that is given in this article. Obtaining homogenized composite characteristics and creating the RVE are

both accomplished via the use of constituent properties and micrographs. The results of the macroscopic simulation are utilized to determine the crucial position, and the node displacements at that site are used as a load case for the RVE in order to analyze the impact that porosity has on the strength of the beam. Validation via experimentation is carried out at each phase.

2.1. Constituent Properties

An industrial manufacturing factory used a heated pultrusion die in order to make the carbon fiber reinforced plastic (CFRP) rods. Standard modulus (high strength) polyacrylonitrile-based (PAN) carbon fiber reinforcement and epoxy resin matrix are the components that make up the composite. The constituent characteristics that were provided by the CFRP manufacturer were used in this work, which is a source that is often utilized in modeling publications [34,35]. A total of two Young's moduli, E1 and E2, as well as one shear modulus, G12, and two Poisson's ratios, ν12 and ν23, are used in this research. The following are the material constants that are most likely to be obtained by experimental means. "1" is used to indicate the direction of the fibers, while "2-3" is used to indicate the transverse plane.

The experimental verification of the qualities of the constituents that were provided was carried out utilizing instrumented nanoindentation whenever it was practicable to do so. Indentation was carried out on longitudinal and transverse cross-sections of the UD CFRP material with the purpose of validating E1f, E2f, and Em. The subscripts "f" and "m" stand for fiber and matrix, respectively. The indentation was carried out using a CSM Instruments
MCT tester (Needham, Massachusetts, United States of America). along order to get ten measurements, specimen cross-sections were wet sanded to a grit of FEPA P4000. These measurements were taken along a line with intervals of 10 µm. Due to the fact that the indentation modulus stabilizes at relatively high values [14, 36, 37], a depth of 0.1 µm was chosen for the indentation. On the other hand, deeper indentation was avoided in order to reduce the risk of fracture and maintain the continuity of the area function of the sphero- conical tip. After analyzing the data, it was clear which indentations had made contact with the fiber and which were located on the matrix. It was determined that the direction of the measurement line for the transverse sample was perpendicular to the direction of the fiber, which indicates that no two measurements were taken from the same filament. The settings for the indentation process are as follows: the indenter is a sphero-conical SB-B28, the tip radius is 2 µm, the cone full angle is 90°, the indentation depth is 0.1 µm, the loading rate is
0.8 mN/min, the dwell period is 30 seconds, and the data collection rate is 10 Hz.

Using the force-displacement data, the first unloading slope was calculated and established. Due to the fact that the power-law fit that is generally used and that was presented by Oliver and Pharr [38] did not generate high-correlation fits, a quadratic polynomial was taken into consideration. It was necessary to remove any permanent displacement (hf) from the data, and then it was necessary to impose intersection with the origin. For the purpose of determining the initial unloading slope, also known as contact stiffness, S [39], the derivative of the polynomial fit at maximum displacement was used. For the purpose of calculating the contact depth (hc), the contact stiffness was used, and the value ε was set to 0.75, as suggested in reference [38]. Calculating the projected contact area and, thus, the indentation modulus M according to Vlassak's definition [40] required the use of the contact depth while doing so. When it is known what the parameters of the indenter are, it is simple to compute the indentation modulus of the isotropic matrix by utilizing the Oliver and Pharr technique [38]. In the case of an anisotropic material, where the contact area is circular, a different solution is used [41, 42]. In this case, the concept is to solve all five stiffness constants by using a five-equation system. This is accomplished by including three previously known stiffness constants and two perpendicular indentation results via the system. The findings of a one-at-a-time sensitivity analysis revealed that none of the engineering constants that were added had a substantial impact on the outcomes on their own. For the purpose of the sensitivity analysis, each engineering constant was gradually increased or decreased by a factor of two or one-half. The values that were obtained for E2f were kept within a deviation of ten percent from the reference scenario. It was the indentation modulus that had the most significant impact, and its relationship was very close to being linear.

2.2. Microstructure

Because a strength model is the end aim in this situation, the morphology of the model is generated by using the

actual microstructure of a pultruded carbon fiber reinforced plastic beam. In order to examine the pultruded carbon fiber reinforced plastic material, high- resolution X-ray microtomography was performed [16]. However, it was discovered that the microtomography voxel data could not be used to differentiate between fiber and matrix, and as a result, a 2.5D technique was chosen. There is an assumption that the fibers are completely straight, despite the fact that the CT data [16] and transverse cross-sections [3]
show that there is some fiber waviness. A Hitachi SU1510 variable pressure scanning electron microscope (VP-SEM) from Tokyo, Japan was used for imaging of two-dimensional cross-sections, and backscatter electron (BSE) detection was utilized for the imaging process. To get a larger yield of back-scattered electrons in comparison to lesser acceleration voltages, the incoming electrons were accelerated with a potential of 25 kV. This was done in order to achieve the desired result. Additionally, a binary color map and manually modified threshold criteria are used in order to conduct an analysis of the fiber volume fraction derived from that picture. By introducing water to the resin bath at the pultrusion line, defects were introduced into the material that was the result of the pultrusion process. Because of the different densities of water and resin, heterogeneous dispersion, and the continuous nature of the pultrusion process, it is impossible to regulate the pore content that is produced as a consequence. As a consequence of this, optical microscopy was required in order to quantify the typically occurring pore size and the pore content that was produced. The photographs were captured with a Nikon Digital Sight DS-U1 camera, which had a resolution of 1600 × 1200 pixels. The microscope utilized was a Nikon Epiphot 200, which was manufactured in Tokyo, Japan. When it comes to the microstructure that contains pores, the 2.5D method of producing a 3D mesh does not permit the use of direct image-based meshing. An section of the microstructure that is abundant in resin is used instead in order to symbolize the impact of porosity.

The experimental verification of the qualities of the constituents that were provided was carried out utilizing instrumented nanoindentation whenever it was practicable to do so. Indentation was carried out on longitudinal and transverse cross-sections of the UD CFRP material with the purpose of validating E1f, E2f, and Em. The subscripts "f" and "m" stand for fiber and matrix, respectively. The indentation was carried out using a CSM Instruments MCT tester (Needham, Massachusetts, United States of America). along order to get ten measurements, specimen cross-sections were wet sanded to a grit of FEPA P4000. These measurements were taken along a line with intervals of 10 µm. Due to the fact that the indentation modulus stabilizes at relatively high values [14,36, 37], a depth of 0.1 µm was chosen for the indentation. On the other hand, deeper indentation was avoided in order to reduce the risk of fracture and maintain the continuity of the area function of the sphero-conical tip. After analyzing the data, it was clear which indentations had made contact with the fiber and which were located on the matrix. It was determined that the direction of the measurement line for the transverse sample was perpendicular to the direction of the fiber, which indicates that no two measurements were taken from the same filament. The settings for the indentation process are as follows: the indenter is a sphero-conical SB-B28, the tip radius is 2 µm, the cone full angle is 90°, the indentation depth is 0.1 µm, the loading rate is 0.8 mN/min, the dwell period is 30 seconds, and the data collection rate is 10 Hz.

Using the force-displacement data, the first unloading slope was calculated and established. Due to the fact that the power-law fit that is generally used and that was presented by Oliver and Pharr [38] did not generate high-correlation fits, a quadratic polynomial was taken into consideration. It was necessary to remove any permanent displacement (hf) from the data, and then it was necessary to impose intersection with the origin. For the purpose of determining the initial unloading slope, also known as contact stiffness, S [39], the derivative of the polynomial fit at maximum displacement was used. For the purpose of calculating the
contact depth (hc), the contact stiffness was used, and the value ε was set to 0.75, as suggested in reference [38]. Calculating the projected contact area and, thus, the indentation modulus M according to Vlassak's definition [40] required the use of the contact depth while doing so. When it is known what the parameters of the indenter are, it is simple to compute the indentation modulus of the isotropic matrix by utilizing the Oliver and Pharr technique [38]. In the case of an anisotropic material, where the contact area is circular, a different solution is used [41,42]. In this case, the concept is to solve all five stiffness constants by using a five-equation system. This is accomplished by including three previously known stiffness constants and two perpendicular indentation results via the system. The findings of a one-at-a-time sensitivity analysis revealed that none of the engineering constants that were added had a substantial impact on the outcomes on their own. For the purpose of the

sensitivity analysis, each engineering constant was gradually increased or decreased by a factor of two or one-half. The values that were obtained for E2f were kept within a deviation of ten percent from the reference scenario. It was the indentation modulus that had the most significant impact, and its relationship was very close to being linear.

3. Results

When the simulation is finished, the results are given in the following order. To begin, the values that were measured are compared to the component qualities that were provided by the manufacturer. In addition, the micrographs that were used for meshing are given. Once the composite characteristics have been obtained, the second step is to generate the representative microstructure and then homogenize it. A comparison is made between the findings produced by analytical and experimental approaches on the other hand. Third, in order to generate loads that are relevant to the micromechanical model, macroscale simulations are brought into play. Lastly, carbon fiber reinforced plastic (CFRP) components are put through a failure test and compared to the simulated stresses and strains of the microstructures that correspond to them.

3.1. Constituent Properties

Within the micromodel, the component attributes and the microstructure are considered to be inputs. A list of material values for the constituents has been supplied by the manufacturer. As a result of the fact that this work only makes use of a single shear modulus, it is necessary to compute v23f by making use of the value of G23f that has been provided, taking into account the isotropic requirement.

For the purpose of verifying a few of the parameters that were provided, nanoindentation was carried out (Figure 4:1). The values that were supplied by the composite manufacturer are significantly different from the Young's moduli that were found from the indentation data (Table 2). [50] It has been claimed that nanobuckling and compressive failure in the nanostructure of carbon fiber are the reasons for the different behavior that might be seen in the case of the fiber. There have been other researchers that have got comparable outcomes for carbon fibers based on polyacrylonitrile [37,51,52,53]. The resultant E2f from these indentations is 13 GPa, which is in the middle of the 20 GPa that was provided by the manufacturer and the inverse micromechanics [14,17] that indicated that E2f should be 10
GPa during transverse compression testing. It is believed that the limitation that is imposed by the fibers that surround the epoxy is the cause of the different epoxy stiffness [53].

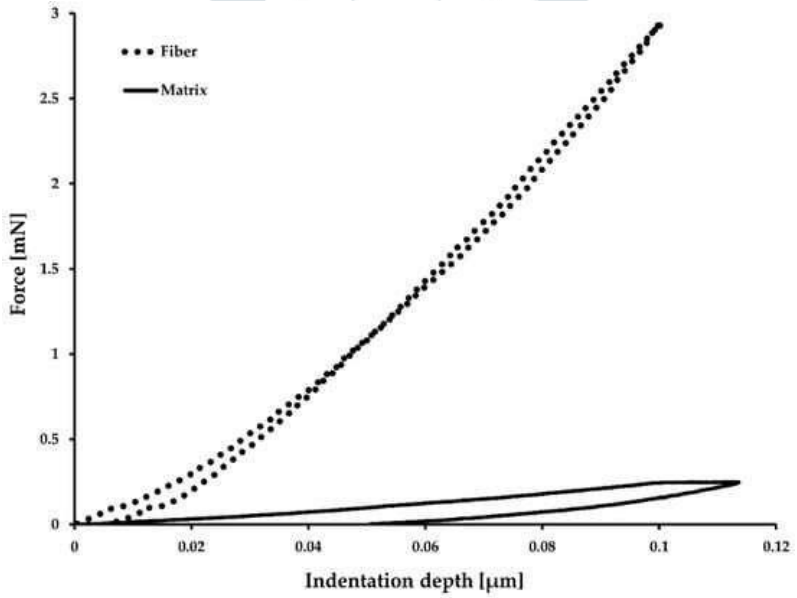

4.2 Effect of Defects

Utilizing the boundary conditions that were acquired from the macroscale hot spot analysis is the last stage in the multiscale modeling technique. This phase involves loading an RVE with a defect that is already discovered. A region of the microstructure that is abundant in resin is used to characterize the microstructure that has porosity. The absence of reinforcing fibers results in a localized increase in strain, and the fibers that are in close proximity to the area are required to bear the load. The flexural strength that was assessed, on the other hand, was not negatively impacted by this particular form of matrix fault. Porosity, on the other hand, leads to a reduction in the shear strength of the CFRP material, and failure occurs in the center plane (1-3) of the specimen, according to apparent ILSS testing. The influence of the resin-rich zone may be seen by modifying the RVE load scenario such that it corresponds with the failure site that was seen in the ILSS testing and then looking at the shear strain components. To be predicted, heterogeneities in the microstructure are responsible for local impacts, which may be evaluated by using the modeling technique that is provided in this article.

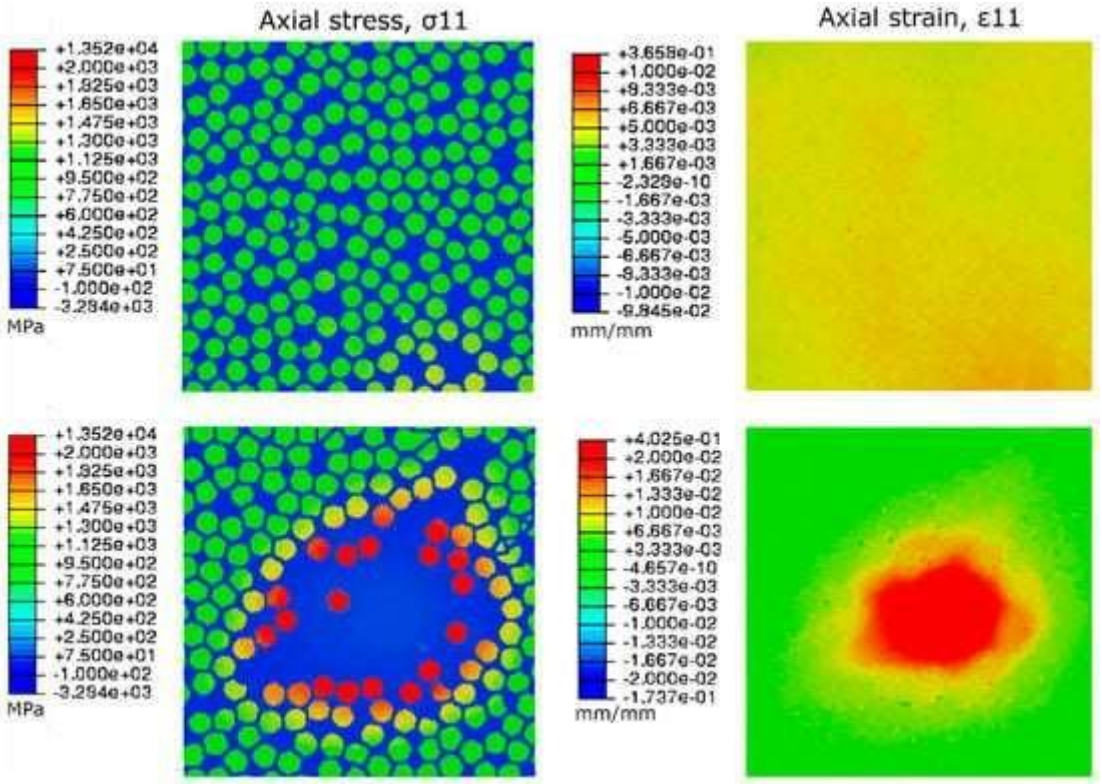

Figure 3. Comparison of reference microstructure (**top**) and resin-rich defect (**bottom**) in tension-dominated loading.

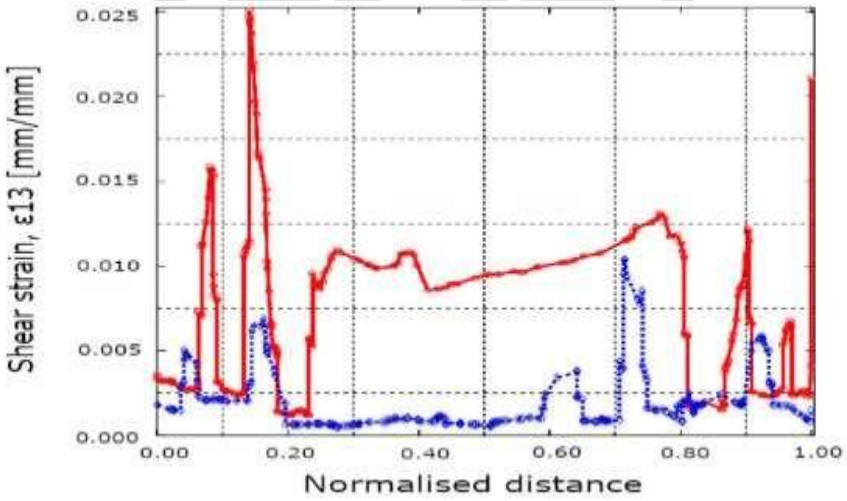

Figure 4. Line plots of the shear strains at the center (red) of the resin-rich microstructure and at the bottom (blue) in a shear-dominated load case.

4. Conclusion

To assess the impact of flaws on unidirectional carbon fiber composites, a micromechanics-based model was developed. Inputs for this model include fiber and resin characteristics, microstructure, macroscale loading conditions, boundary conditions, and defect design and location. However, caution is warranted when accepting

manufacturer-indicated fiber and resin qualities due to unknown measurement techniques. Nanoindentation, particularly for determining longitudinal fiber and matrix properties, yields unsatisfactory results. Possible explanations for this discrepancy include nanoscale bending of the fiber and a constraint effect in the matrix. Comparatively, transverse nanoindentation results were more aligned with inverse micromechanics solutions and literature values of functionally equivalent fibers. Despite ambiguity in input parameters, homogenized composite characteristics closely matched experimental verifications. To represent the microstructure, SEM images were successfully segmented using an algorithm to generate a mesh. However, two-dimensional micrographs neglect fiber waviness effects and defect morphology. Macroscale simulations showed excellent agreement with actual data, both in terms of elastic response and failure site. A sensitivity analysis revealed that the only factor substantially impacting macroscale response is the longitudinal modulus of the composite material. Moreover, the longitudinal fiber modulus, often unknown, is the primary factor influencing this value. Transverse characteristics have minimal impact, with an assumption of isotropic material properties resulting in only a three percent error in stress/strain relationships. Only three-point bending was utilized as a load instance

5. References

[1] Rizzo, P.; di Scalea, L. Acoustic emission monitoring of carbon-fiber-reinforced-polymer bridge stay cables in large-scale testing. Exp. Mech. 2001, 41, 282–290. [Google Scholar] [CrossRef]

[2] Rebel, G.; Verreet, R.; Ridge, I.M.L. Lightweight ropes for lifting applications. In Proceedings of the OIPEEC Conference, Athens, Greece, 27–29 March 2006; pp. 33–54. [Google Scholar]

[3] Antin, K.-N.; Machado, M.A.; Santos, T.G.; Vilaça, P. Evaluation of different non- destructive testing methods to detect imperfections in unidirectional carbon fiber composite ropes. J. Nondestruct. Eval. 2019, 38, 23. [Google Scholar] [CrossRef]

[4] Machado, M.A.; Antin, K.-N.; Rosado, L.S.; Vilaça, P.; Santos, T.G. Contactless high-speed eddy current inspection of unidirectional carbon fiber reinforced polymer. Compos. Part B Eng. 2019, 168, 226–235. [Google Scholar] [CrossRef]

[5] Hedgepeth, J.M.; van Dyke, P. Local stress concentrations in imperfect filamentary composite materials. J. Compos. Mater. 1967, 1, 294–309. [Google Scholar] [CrossRef]

[6] Landis, C.M.; McMeeking, R.M. Stress concentrations in composites with interface sliding, matrix stiffness and uneven fiber spacing using shear lag theory. Int. J. Solids Struct. 1999, 36, 4333–4361. [Google Scholar] [CrossRef]

[7] Otero, J.A.; Rodriguez-Ramos, R.; Bravo-Castillero, J.; Guinovart-Diaz, R.; Sabina, F.J.; Monsivais, G. Semi-analytical method for computing effective properties in elastic composite under imperfect contact. Int. J. Solids Struct. 2013, 50, 609–622. [Google Scholar] [CrossRef] [Green Version]

[8] Sun, C.T.; Vaidya, R.S. Prediction of composite properties from a representative volume element. Compos. Sci. Technol. 1996, 56, 171–179. [Google Scholar] [CrossRef]

[9] Mishnaevsky, L., Jr.; Broensted, P. Micromechanical modeling of damage and fracture of unidirectional fiber reinforced composites: A review. Comput. Mater. Sci. 2009, 44, 1351– 1359. [Google Scholar] [CrossRef]

[10] Wongsto, A.; Li, S. Micromechanical FE analysis of UD fibre-reinforced composites with fibres distributed at random over the transverse cross-section. Compos. Part A 2005, 36, 1246–1266. [Google Scholar] [CrossRef]

[11] Dong, C. Effects of Process-Induced Voids on the Properties of Fibre Reinforced Composites. J. Mater. Sci. Technol. 2016, 7, 597–604. [Google Scholar] [CrossRef]

[12] Swolfs, Y.; Gorbatikh, L.; Romanov, V.S.; Orlova, S.; Lomov, S.V.; Verpoest, I. Stress concentrations in an impregnated fibre bundle with random fibre packing. Compos. Sci. Technol. 2013, 74, 113–120. [Google Scholar] [CrossRef]

[13] Vaughan, T.J.; McCarthy, C.T. Micromechanical modelling of the transverse damage behaviour in fibre reinforced composites. Compos. Sci. Technol. 2011, 71, 388–396. [Google Scholar] [CrossRef]

[14] Maurin, R.; Davies, P.; Baral, N.; Baley, C. Transverse properties of carbon fibres by nano-indentation and micro-mechanics. Appl. Compos. Mater. 2008, 15, 61–73. [Google Scholar] [CrossRef]

[15] Beicha, D.; Kanit, T.; Brunet, Y.; Imad, A.; El Moumen, A.; Khelfaoui, Y. Effective transverse elastic properties of unidirectional fiber reinforced composites. Mech. Mater. 2016, 102, 47–53. [Google Scholar] [CrossRef]

[16] Schumacher, D.; Antin, K.-N.; Zscherpel, U.; Vilaça, P. Application of different X-ray techniques to improve in-service carbon fiber reinforced rope inspection. J. Nondestruct. Eval. 2017, 36, 1–14. [Google Scholar] [CrossRef]

[17] Halpin, J.C.; Kardos, J.L. The Halpin-Tsai equations: A review. Polym. Eng. Sci. 1976, 16, 344–352.

[Google Scholar]
[18] Sarlin, E.; von Essen, M.; Palola, S.; Lindgren, M.; Kallio, P.; Vuorinen, J. Determination of environmental degradation of matrix and fiber materials with a novel, stastically reliable micro-robotic approach. In Proceedings of the 17th European Conference on Composite Materials ECCM17, München, Germany, 26–30 June 2016. [Google Scholar]
[19] Ilankeeran, P.K.; Mohite, P.M.; Kamle, S. Axial tensile testing of single fibres. Mod. Mech. Eng. 2012, 2, 151–156. [Google Scholar] [CrossRef]
[20] Chamis, C.C. Simplified composite micromechanics equations for hygral, thermal and mechanical properties. NASA Technical Memorandum 83320. In Proceedings of the 38th Annual Conference of the Society of the Plastics Industry, Houston, TX, USA, 7–11 February 1983. [Google Scholar]
[21] Mounier, D.; Poilane, C.; Bucher, C.; Picart, P. Evaluation of transverse elastic properties of fibers used in composite materials by laser resonant ultrasound spectroscopy. In Proceedings of the Acoustics Conference, Nantes, France, 23–27 April 2012. [Google Scholar]
[22] Soden, P.D.; Hinton, M.J.; Kaddour, A.S. Lamina properties, lay-up configurations and loading conditions for a range of fibre-reinforced composite laminates. Compos. Sci. Technol. 1998, 58, 1011–1022. [Google Scholar] [CrossRef]
[23] Turon, A.; Costa, J.; Maimi, P.; Trias, D.; Mayugo, J.A. A progressive damage model for unidirectional fibre-reinforced composites based on fibre fragmentation. Part I: Formulation. Compos. Sci. Technol. 2005, 65, 2039–2048. [Google Scholar] [CrossRef]
[24] Blassiau, S.; Thionnet, A.; Bunsell, A.R. Micromechanisms of load transfer in a unidirectional carbon fibre–reinforced epoxy composite due to fibre failures. Part 1: Micromechanisms and 3D analysis of load transfer: The elastic case. Compos. Struct. 2006, 74, 303–318. [Google Scholar] [CrossRef]
[25] Behzadi, S.; Jones, F.R. The effect of temperature on stress transfer between a broken fibre and the adjacent fibres in unidirectional fibre composites. Compos. Sci. Technol. 2010, 68, 2690–2696. [Google Scholar] [CrossRef]
[26] Bouaoune, L.; Brunet, Y.; El Moumen, A.; Kanit, T.; Mazouz, H. Random versus periodic microstructures for elasticity of fibers reinforced composites. Compos. Part B 2016, 103, 68–
73. [Google Scholar] [CrossRef]
[27] Melro, A.R.; Camanho, P.P.; Pinho, S.T. Generation of random distribution of fibres in long- fibre reinforced composites. Compos. Sci. Technol. 2008, 68, 2092–2102. [Google Scholar] [CrossRef]
[28] Swolfs, Y.; Verpoest, I.; Gorbatikh, L. Issues in strength models for unidirectional fibre- reinforced composites related to Weibull distributions, fibre packings and boundary effects. Compos. Sci. Technol. 2015, 114, 42–49. [Google Scholar] [CrossRef] [Green Version]
[29] Okabe, T.; Takeda, N.; Kamoshida, Y.; Shimizu, M.; Curtin, W.A. A 3D shear-lag model considering micro-damage and statistical strength prediction of unidirectional fiber- reinforced composites. Compos. Sci. Technol. 2001, 61, 1773–1787. [Google Scholar] [CrossRef]
[30] Trias, D.; Costa, J.; Mayugo, J.A.; Hurtado, J.E. Random models versus periodic models for fibre reinforced composites. Comput. Mater. Sci. 2006, 38, 316–324. [Google Scholar] [CrossRef]
[31] Holmberg, K.; Laukkanen, A.; Turunen, E.; Laitinen, T. Wear resistance optimisation of composite coatings by computational microstructural modelling. Surf. Coat. Technol. 2014, 247, 1–13. [Google Scholar] [CrossRef]
[32] Orell, O.; Vuorinen, J.; Jokinen, J.; Kettunen, H.; Hytönen, P.; Turunen, J.; Kanerva, M. Characterization of elastic constants of anisotropic composites in compression using digital image correlation. Compos. Struct. 2018, 185, 176–185. [Google Scholar] [CrossRef]
[33] Haj-Ali, R.; Kilic, H. Nonlinear constitutive model for pultruded FRP composites. Mech. Mater. 2003, 35, 791–801. [Google Scholar] [CrossRef]
[34] Fiedler, B.; Holst, S.; Hobbiebrunken, T.; Hojo, M.; Schulte, K. Modelling of the initial failure of CFRP structures by partial discretisation: A micro/macro-mechanical approach of first ply failure. Adv. Compos. Lett. 2004, 13. [Google Scholar] [CrossRef]
[35] Fliegener, S.; Luke, M.; Gumbsch, P. 3D microstructure modeling of long fiber reinforced thermoplastics. Compos. Sci. Technol. 2014, 104, 136–145. [Google Scholar] [CrossRef]
[36] Miyagawa, H.; Mase, T.; Sato, C.; Drown, E.; Drzal, L.T.; Ikegami, K. Comparison of experimental and theoretical transverse elastic modulus of carbon fibers. Carbon 2006, 44, 2002–2008. [Google Scholar] [CrossRef]